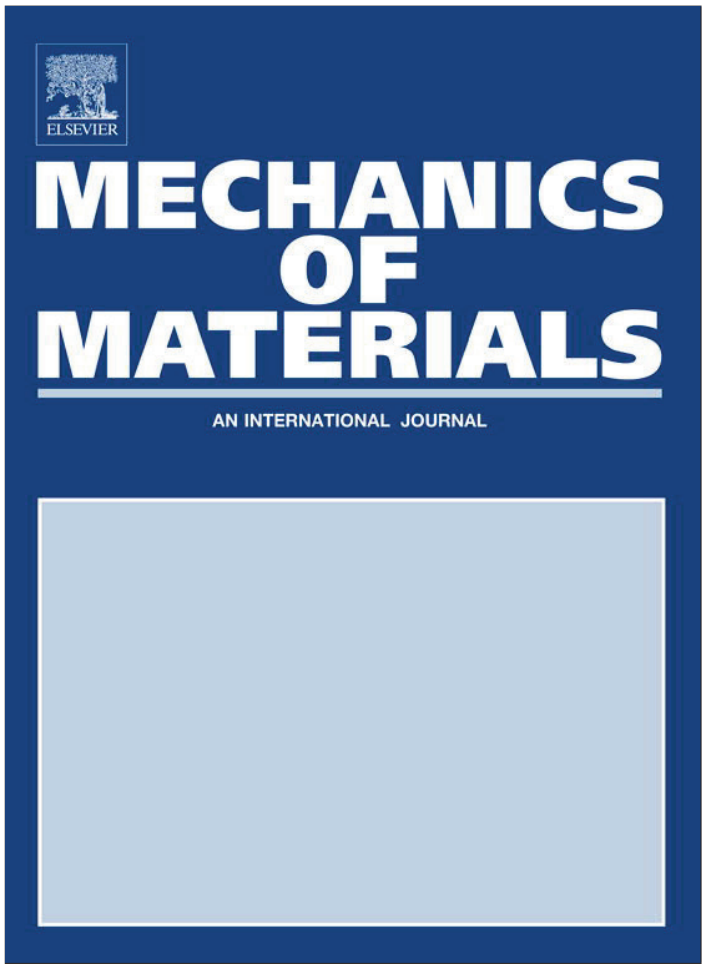

(This is a sample cover image for this issue. The actual cover is not yet available at this time.)

Mechanics of Materials 54 (2012) 91–99

Contents lists available at SciVerse ScienceDirect

Mechanics of Materials

journal homepage: www.elsevier.com/locate/mechmat

Static and dynamic flexural strength of 99.5% alumina: Relation to surface roughness

A. Belenky, D. Rittel *

Faculty of Mechanical Engineering, Technion, Israel Institute of Technology, 32000 Haifa, Israel

ARTICLE INFO

Article history:
Received 23 February 2012
Received in revised form 30 May 2012
Available online 17 July 2012

Keywords:
Alumina
Surface roughness
Flexural strength
1-Point impact
Pores

ABSTRACT

The dynamic flexural strength of ceramics is an important property for all applications involving impact loading conditions. Therefore, this work reports a systematic comparison of static and dynamic flexural strength results for 99.5% commercial alumina, obtained using a recently reported adaptation of the 1-point impact experimental technique. Specimens of the same size and *systematically varying* surface roughness conditions were used in this study to assess the influence of the latter on the static and dynamic strength of this material. The investigated roughness levels ranged from 0.8 μm (coarse) to 0.05 μm (fine, polished). Under static loading, reducing the surface roughness causes a 10% increase in flexural strength for polished specimens. By contrast, the dynamic flexural strength is apparently not influenced by the surface roughness. A thorough microstructural and fractographic examination reveals the presence of bulk (surface) pore-like flaws that are not obliterated by the polishing process and therefore govern the failure process. It is suggested that strength improvements can be reached by suitable surface preparation, provided no bulk pores are native in the material, some of which are present on its surface. The identification of the role of surface flaws is expected to clarify the discrepancy found in the literature as to the influence of surface roughness on the mechanical properties of brittle materials.

1. Introduction

Advanced ceramic materials are widely implemented in a variety of cutting edge engineering applications. They are mostly manufactured by powder metallurgy process. One of the main advantages of this manufacturing process is that shapes close to the final one can be easily achieved, thus significantly minimizing the manufacturing costs. Yet, in cases when precise components are required, additional machining is needed. Due to the fact that advanced ceramic materials are very hard, conventional machining methods, e.g. milling and turning are generally not applicable (Bandyopadhyay, 1995). Instead, the common machining methods of advanced ceramics are essentially abrasive, i.e., grinding, polishing, sandblasting. Ceramic materials are essentially brittle and reported to be sensitive to surface conditions. Each machining method leaves its unique surface pattern or even damage, e.g. cracks, or residual stresses. These, in turn, may alter (weaken) the final strength of a ceramic component.

Considering the influence of different manufacturing methods on the strength of ceramic components under static loading conditions, much work has been done. Bandyopadhyay (1995) conducted research for two types of silicon nitride ceramics and assessed how different grinding grit sizes affect the flexural strength. His major finding is that the average flexural strength of both investigated SiN ceramics is not sensitive to grinding parameters, limiting it only to longitudinal grinding. It was recognized by Bandyopadhyay (1995) that for one of the tested materials, the insensitivity is probably caused by a relatively large bulk porosity that was the primary cause for failure. Zheng et al. (2000) showed that there is a correlation between the

* Corresponding author.
E-mail address: merittel@technion.ac.il (D. Rittel).

0167-6636/$ - see front matter © 2012 Elsevier Ltd. All rights reserved.
http://dx.doi.org/10.1016/j.mechmat.2012.07.003

static flexural strength of hot-pressed silicon nitride and the surface finish in their specimens. From their work one may conclude that by reducing significantly the surface roughness, the expected flexural strength values will markedly increase (up to 30%). Liao et al. (1997) conducted research on two grades of 99.5% alumina and commercial silicon nitride ground under different conditions. One of their interesting findings is that for alumina, specimens with better surface finish always showed higher strength, but this was not the case for silicon nitride. Gupta (1980) reports that the strength of ground metastable tetragonal zirconia increases with decreasing grit size (improved surface finish). Other works on ceramic dental materials compared between sandblasting, grinding, polishing and glazing in terms of flexural strength (Albakry et al., 2004; Guazzato et al., 2004). Albakry et al. (2004) concluded that surface roughness may not be the only cause that controls the strength of investigated material, while several factors (residual stresses, porosity, inherently developed cracks) may be more pertinent. Guazzato et al. (2004) report that heat treatment conducted after different surface treatments improves the flexural strength of the investigated dental material (In-Ceram Alumina). The reason for the improvement is that heat treatment caused the glass present in the material to fill up the surface flaws/cracks.

Ritter and Davidge (1984) considered different microstructural and machining-induced defects in ceramics and discussed them based on fracture mechanics considerations. They claimed that for alumina, failure is most likely to develop from a single critical flaw, or by coalescence of several smaller flaws. One of their conclusions was that it is probably impossible to manufacture ceramic materials with a uniform strength, due to complexity in fabrication and failure process. Nakamura et al. (2009) reported that ~85% of his alumina specimens fractured in 4-point bending failed from surface flaws, and that the identification of fracture origins for alumina ceramics is a very difficult task.

All the aforementioned studies concerned static failure. For the dynamic loading case, there is a noticeable scarcity of studies on the influence of surface conditions on the strength of brittle materials. Nevertheless, one should mention the recent works of Nie et al. (2010, 2009) that show an adaptation of 4-point bending test and ring-on-ring equibiaxial flexural strength test to the dynamic loading regime using a modified Split Hopkinson Pressure Bar (SHPB) (Kolsky, 1949). These authors implemented both techniques on testing dynamic flexural strength of borosilicate glass with different surface finishes. The measured surface roughness values of their glass specimens (Ra) were: 0.41, 0.059 and 0.236 μm (Nie et al., 2009). The first two roughness values were achieved by grinding, polishing and the last one by etching (HF acid). Two studies (Nie et al., 2010, 2009) show that the flexural strength of borosilicate glass increases with increasing loading rate for the same roughness conditions. A flexural strength of 1.1 GPa was measured under dynamic loading for chemically etched specimens (1.3 GPa for equibiaxial flexural strength). Additional points from their work (Nie et al., 2009) are that for the ground specimens, the flexural strength decreases with increasing surface roughness, and the surface roughness (Ra) values alone are not sufficient to relate the flexural strength to the surface quality of glass material. The data about increasing strength for a smoother surface of a glass led to the incorporation of a surface characteristic parameter into a recent computational constitutive model for glass by Holmquist and Johnson (2011). Vlasov et al. (2002) reported that under ballistic impact loading, the dominant failure modes are due to spalling and bending-induced tension of the back side of the tested plate, when the latter may be related to surface conditions, without further specifications.

From the above literature survey, it appears that some correlation between the static strength of advanced ceramics and the surface finish does exist, yet not for all ceramic materials, while the origins of the phenomenon are not clearly understood. In the case of dynamic loading, there are no detailed studies, to the best of our knowledge, about the correlation between strength of advanced ceramics and the surface finish.

Quite recently, Belenky and Rittel (2012) investigated the static and dynamic flexural strength of commercial 99.5% alumina, while the surface roughness was kept identical for all the specimens. These authors reported a noticeable increase in strength for the dynamic loading conditions (Belenky and Rittel, 2012). The reasons for this behavior were elucidated by a comparative quantitative fractographic study showing the role of microstructural flaws (collectively termed as porosity) in the failure process. These flaws are native to the material as a result of the fabrication process, and the emphasis was put on those surface and subsurface flaws that initiate fracture.

Consequently, the present study reports a systematic comparative investigation of the static and dynamic strength of a similar commercial 99.5% alumina, in which the surface roughness is systematically varied. The experimental technique adopted in this work is based on a recent adaptation of 1-point impact (Bohme and Kalthoff, 1982) technique for measuring dynamic flexural strength of brittle materials (Belenky and Rittel, 2011).

The paper is organized as follows: firstly the investigated material, specimen geometry, surface roughness measurements and experimental procedures are presented. Next, we report the measured static and dynamic flexural strength values and their correlation to the surface roughness, followed by a detailed comparative fractographic study. The paper ends by a discussion of the main results, followed by concluding remarks.

2. Material and experimental procedures

2.1. Material and specimens

The flexural strength measurements reported in this study were carried out on a commercial grade 99.5% alumina (Bitossi, Italy). The mechanical properties of the evaluated material, as reported by the manufacturer, are given in the first row of Table 1. Rectangular beam specimens ($3 \times 4 \times 45\ mm^3$) were machined according to ASTM-C1161 (1994) recommendations. It should be emphasized

Table 1
Specimens and incident bar material properties.

	Material	Density ρ [kg/m^3]	Young's modulus E [GPa]	Poisson's ratio ν	Flexural strength [MPa]
Specimens (Bitossi)	Alumina 99.5%	3900	370	0.22	379
Incident bar	15–5 PH steel	7800	202	0.3	–

that specimens from the same size were used for both static and dynamic loading regimes (Belenky and Rittel, 2011).

All the specimens were initially ground and chamfered according to the standard recommendations (ASTM-C1161, 1994), and then divided arbitrarily into three groups of 35 specimens each. Specimens from the first groups were left aside. Specimens from the other two groups were additionally ground and polished as follows: one of the wider specimens' faces (4×45 mm^2) from the second and the third groups were machined to Ra levels of 0.4 μm and 0.05 μm, respectively. The surface roughness parameter, Ra, was carefully measured for each and every specimen before testing, three points for each specimen, in the mid-section at the same level of magnification ($\times$25.7), using a Wyko NT1100 optical interferometer (Veeco, USA). During the tests (both static and dynamic), the specimens were positioned in such way that the face with the measured (controlled) roughness was deformed in tension. In other words, all the specimens had varying surface conditions on their tensile faces. Prior to testing, all the specimens were examined under the optical microscope in order to detect any handling damage or visible cracks, and specimens that were found suspicious were not tested at all. At least 14 valid tests were obtained under each loading regime for each group. All the tests were carried out at ambient environmental conditions, namely a temperature of 24 ± 3 °C and relative humidity of 45 ± 4%.

2.2. Static flexural tests

The specimens were fractured in three-point bending with a roller span of 40 mm, at a constant crosshead velocity of 0.5 mm/min using a screw-driven universal testing machine (Instron 4483, Instron, USA), with a 500 N load cell. The flexural strength values were extracted from the maximum load, according to the standard recommendations (ASTM-C1161, 1994).

In order to measure and validate the Young's modulus of the investigated material, strain gauges were glued on a tensile face of six specimens, two specimens from each group and then fractured. An average value of measured Young's modulus was found to be in excellent agreement with this reported by the manufacturer, Table 1.

2.3. Dynamic flexural tests

Dynamic flexural strength results measured in the present work were obtained using a recently reported modification of the 1-point impact experimental technique. This technique is based on Split Hopkinson Pressure Bar (Kolsky, 1949) and utilizes the incident bar only, as was previously reported by other authors who used 1-point impact technique, mostly for measuring dynamic fracture toughness (Belenky et al., 2010; Kalthoff, 1986; Weisbrod and Rittel, 2000). The major difference in the present technique is that the specimens are not notched or precracked, thus allowing to measure the flexural strength instead of the dynamic fracture toughness. Several observations are greatly simplifying the implementation of the 1-point impact technique for strength measurement purposes. First, under 1-point impact conditions, the specimen's failure is primarily due to its inertia, so that the specimens do not need to be supported, which in turn greatly facilitates modeling. It should also be noted that the approach adopted in this work is of a hybrid experimental–numerical nature, in which the actual boundary conditions and fracture time from the test are applied to a linear elastic numerical (finite element (ABAQUS, 2010)) model of the experiment in order to calculate the dynamic flexural strength. Numerical modeling, calculation procedures and the accuracy of used technique are all thoroughly discussed in our previous work (Belenky and Rittel, 2011).

Prior to the tests, silver paint fracture gauges were silk-screened on the outer (tensile) surface of each specimen. The incident bar used in this study was made from PH 15-5 steel, whose mechanical properties are listed in Table 1, with a diameter of ø6.35 mm and length of 660 mm. The strain gauges were positioned at 400 mm from the end of the incident bar that is in contact with

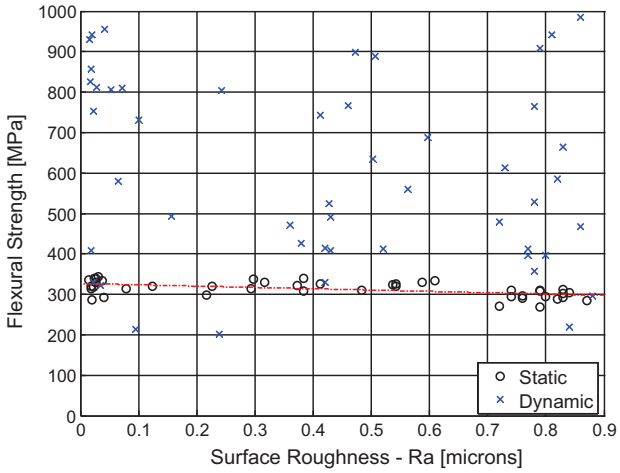

Fig. 1. Measured static and dynamic flexural strength values vs. surface roughness parameter (Ra) for the investigated material. The fitted line shows the general trend only for static flexural strength measurements. According to fitted line there is a ~10% increase in flexural strength for lower Ra values (polished specimens) for static loading. The dynamic flexural strength values do not lead to a meaningful correlation with the surface roughness.

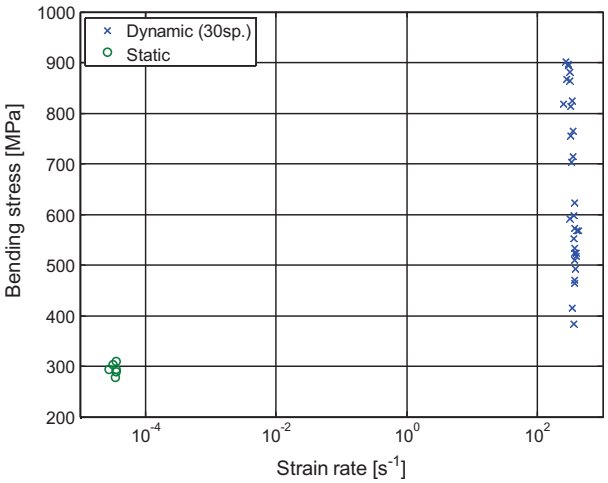

Fig. 2. Comparison of flexural strength results for static and dynamic loading regimes vs. strain-rate for another commercial 99.5% alumina (CoorsTech, USA), reprinted from Belenky and Rittel (2012). The strain-rates are similar to measured in the present study. The surface roughness (Ra) of specimens used in the previous study was 0.9 ± 0.15 μm.

the specimen. The pressure levels that propel the striker and the striker's length were kept constant during all the tests, meaning an almost similar strain-rate, as was reported in a previous work (Belenky and Rittel, 2012). All the signals, namely strain and fracture gauge signals, were synchronized with the incident strain gauge signal, as shown previously (Belenky and Rittel, 2011).

3. Experimental results

3.1. Flexural strength results

The measured values of static and dynamic flexural strength vs. surface roughness parameter (Ra) of the investigated material are shown in Fig. 1. The fitted line, to the static flexural strength results, is showing the general trend only. It should be emphasized that because of the large scatter in the dynamic loading results, no trend line was fitted. The static flexural strength values, measured in the present work, are in very good agreement with our previous study on commercial 99.5% alumina (Belenky and Rittel, 2012), but again, somewhat lower that those reported by the manufacturer, Table 1. Yet, according to the fitted trend line, there is an apparent 10% increase in the static flexural strength for polished specimens (lower Ra values). Dynamic flexural strength, as shown in Fig. 1, is significantly higher than its static counterpart, showing again a very good agreement with the previous observations (Belenky and Rittel, 2012), which are shown here in Fig. 2. From the flexural strength measurement reported in the present work, no reliable estimations of the Weibull distribution parameters can be made, both in static and dynamic loading regimes. The reasons for that are that all the specimens had a varying surface roughness, precluding a significant statistical analysis. But even if this was not the case and all the specimens within each group were identical, we suspect that the sample size of each specimen's group is still too small for reliable Weibull

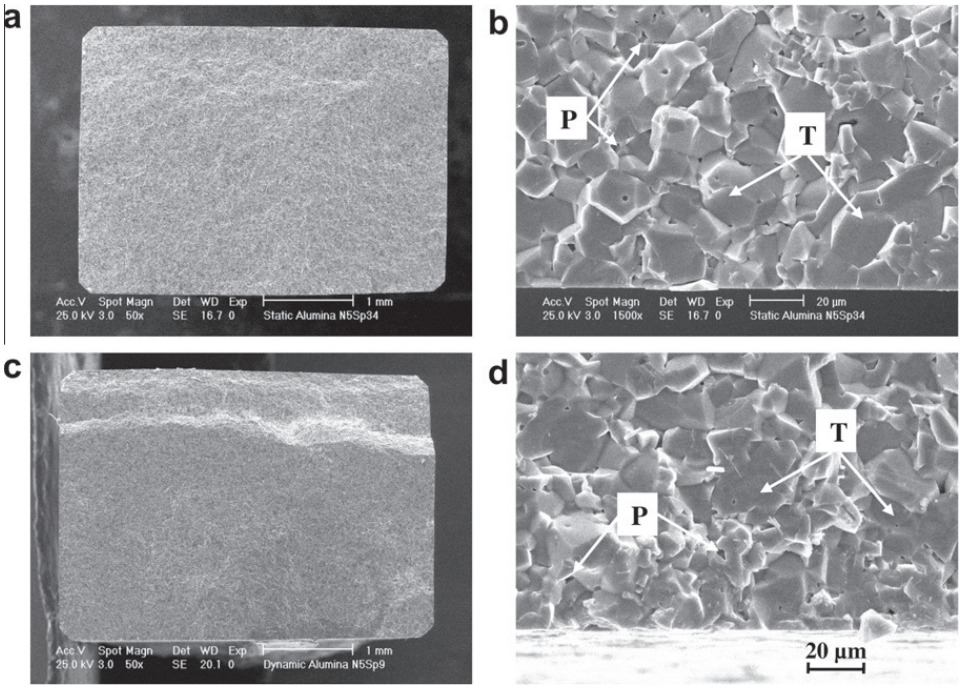

Fig. 3. Comparison of fractographic pictures of statically and dynamically broken specimens, at two magnification levels (×50 and ×1500). The bottom edge in all pictures is the tensile faces. "T" stands for transgranular failure mechanism; "P" stands for pores. a and b: Statically broken specimen (N5Sp34), at lower magnification no distinct failure origin can be identified; at higher magnification: the failure mechanism is predominantly transgranular with minor pullouts. c and d: Dynamically broken specimen (N5Sp9), at lower magnification fracture surface seems to be fairly similar to the static one, again - no distinct failure origin; at high magnification: the failure mechanism is again predominantly transgranular with minor grain pullouts (intergranular).

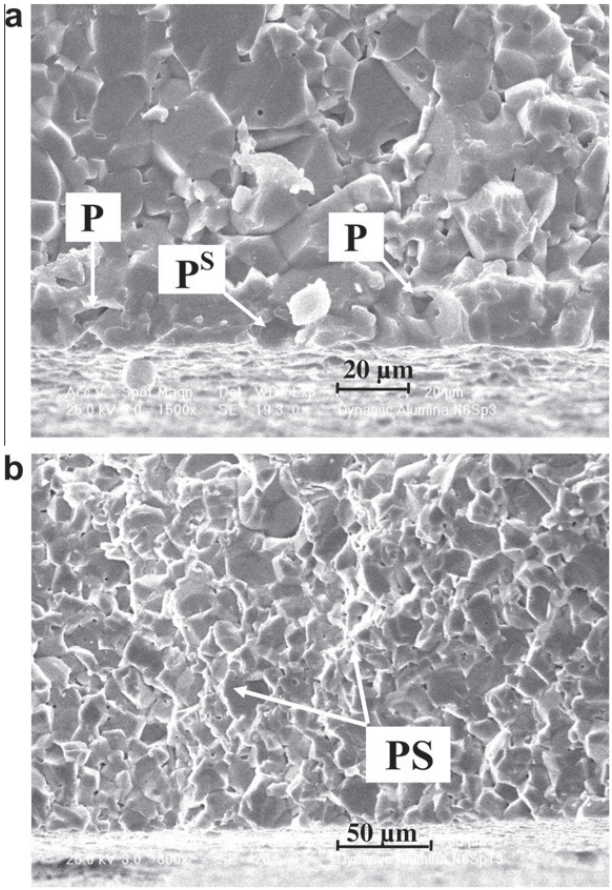

Fig. 4. Strength limiting defects that were identified on the fracture surfaces of dynamically broken specimens that correlated to extremely lower values of dynamic flexural strength. The bottom edge in both pictures is the tensile faces: (a) Surface pore (P^S) and several relatively large subsurface pores (P), resulting dynamic flexural strength is 413.3 MPa (×1500N6Sp3) and (b) Porous seam (PS), resulting dynamic flexural strength is 297.0 MPa (×800N6Sp13).

distribution parameters calculations. A marked strain-rate sensitivity is present for all the investigated surface roughness conditions. The dynamic flexural strength, although higher than the quasi-static, does not reveal a clear correlation with the surface roughness of the specimen. One should also note that the high scatter in the dynamic tests is a constant feature that was repeatedly observed in this as well as in the previous work.

3.2. Fractographic study

In order to understand the causes for the differences in measured static and dynamic flexural strength values, a detailed comparative fractographic study was conducted. Several specimens were gold coated and fracture surfaces were examined using the Scanning Electron Microscope (Philips XL 30). Selected typical fractographs are shown in Fig. 3. Fig. 3a and b shows the fracture surface of a specimen broken under quasi-static loading at ×50 and ×1500 magnification levels, respectively. At lower magnification (Fig. 3a), no distinct failure origin can be identified. At higher magnifications (Fig. 3b), the failure mechanism is predominantly transgranular with a minor component of grains pullout (intergranular cracking). The same conclusions were reached for the fracture surfaces of dynamically broken specimen, Fig. 3c and d. At lower magnification, Fig. 3c, no distinct failure origin can be identified. At higher magnification the failure mechanism is again predominantly transgranular with a minor component of grains pullout. Nakamura et al. (2009) mentioned that identification of failure origins for alumina ceramics is a very difficult task, and this is indeed the case here. In addition, a significant number of pores is clearly seen on both the static and dynamic fracture surfaces, a point that is in good agreement with our previous work on similar material (Belenky and Rittel, 2012). It should be mentioned that many more fracture surfaces were examined, leading to the same conclusions. Similar observations of predominantly transgranular fracture mechanism were already reported for other grades of alumina (Gálvez et al., 2000) under dynamic loading.

In addition, several specimens that showed a significantly lower dynamic flexural strength were especially investigated by means of SEM. It was found that those specimens, with extremely low dynamic flexural strength values (outliers), had in most cases a distinct fracture origin (flaw), which could not be identified for those with a high fracture strength. Examples of such strength limiting flaws are shown in Fig. 4. In Fig. 4a a large surface pore (marked P^S) along with several adjacent subsurface pores are clearly seen. Another strength limiting defect that was identified on several fracture surfaces, and caused extremely low dynamic flexural strength values is a porous seam (PS), marked on Fig. 4b. The terminology for strength limiting flaws used here is according to ASTM-C1322 (2005) standard. Such low strength values, even caused by an unusual defect, still should be considered in case of a design consideration or statistical analysis.

The flexural strength results measured in this study showed a relatively weak correlation between the flexural strength and surface roughness, much less than was expected or reported so far in the literature for other brittle materials (Nie et al., 2009; Zheng et al., 2000). So, additional study of fracture surfaces, including surface roughness conditions, was carried out, as shown in Figs. 5–7. Fig. 5 shows a specimen that was ground to Ra level of 0.80 μm. Figs. 6 and 7 show specimens that were ground and polished to Ra levels of 0.217 and 0.027 μm, respectively. Fig. 5b shows an SEM picture of the tensile face (TF). Even though the specimen was ground according to the standard requirements (ASTM-C1161, 1994), there are many surface features along with several valleys (pores). However, the presence of the latter on the specimen's surface is not that pronounced. Fig. 5c was taken by optical profilometer and shows the same surface. In this picture the presence of pores along with surface heights distribution is clearly seen. In Fig. 6b one can see the tensile face of a specimen that was treated to a surface roughness level of Ra 0.217 μm. An interesting feature shown in this figure is that, although the surface is nominally flatter, the presence of pores on the specimen's surface is more pronounced. This point can be easily accessed by checking surface features as was identified by optical profilometery, Fig. 6c. First, as shown by the heights distribution color bar,

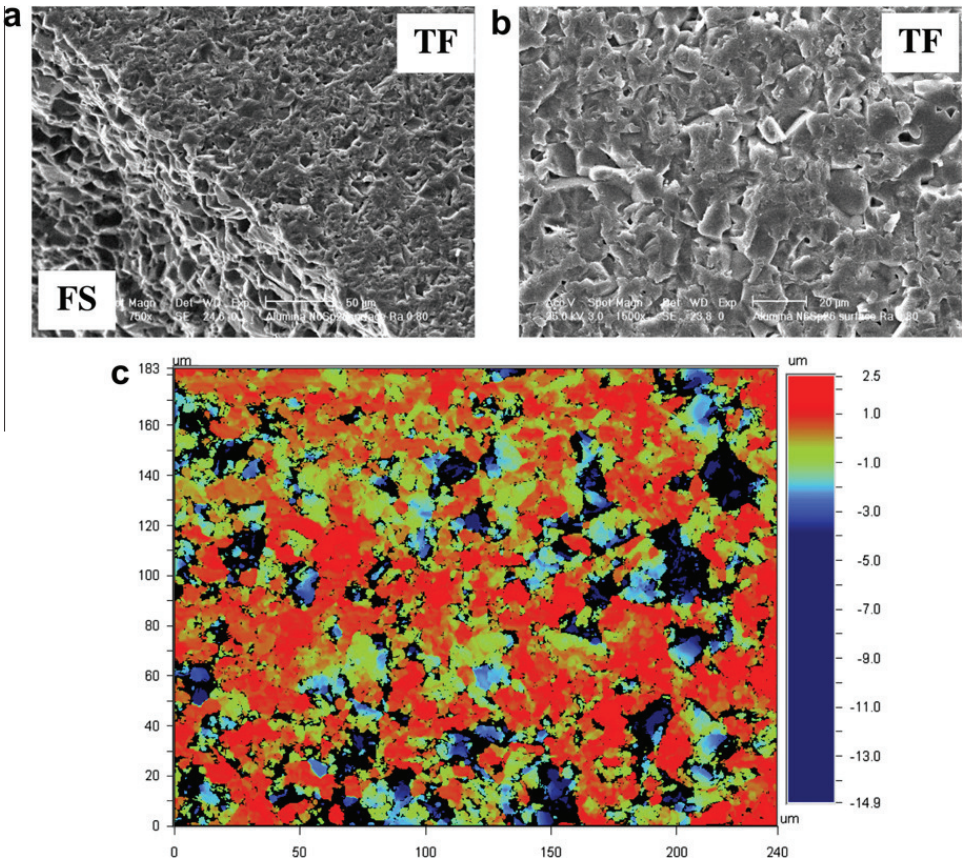

Fig. 5. SEM and optical profilometer images of specimen's surface treatment (grinding) to a level of Ra 0.8 μm. TF stands for a tensile face, FS is a fracture surface: (a) Close up on the tensile face and the fracture surface (SEM, ×750), (b) Surface features left after grinding the specimen to a Ra level of 0.8 μm (SEM, ×1500). and (c) Surface features map as was identified by optical profilometer, the color bar range is from 2.5 to −14.9 μm (×25.7).

the surface is indeed flatter, comparing to the one, shown in Fig. 5c. Secondly, the grinding direction is clearly seen. If one compares between Fig. 6b and c, it can be seen that not all valleys are indeed pores. Some of the additional surface features shown in Fig. 6b can be grain boundaries, revealed by the surface treatment or just cavities left from tearing some grains apart from the specimen's surface during grinding. Fig. 7b shows an SEM picture of tensile face of a specimen that was polished to a surface roughness level of Ra 0.027 μm. From this picture it seems that, even after thorough polishing, a significant level of residual porosity is still detected on the surface of the specimen. By checking Fig. 7c, polishing scratches are clearly seen, in addition to a significant number of pores.

The main finding from Figs. 5 to 7 is that, irrespective of the surface treatment or roughness of the tensile face, surface porosity (flaws) is inherently detected in the investigated material. This observation strongly suggests that the surface porosity actually controls the flexural strength of the material, rather than its surface condition. This point can be further assessed by checking Figs. 5–7a. In Figs. 5–7a a close up on the tensile face (TF) along with part of fracture surface (FS) is shown, at the same level of magnification (×750, SEM). If one virtually tracks after the crack path on the edge between the tensile face and fracture surface, it can be seen that for a rougher tensile face (Fig. 5a) no distinct conclusion can be made. Yet, for smoother tensile faces, as can be seen in Figs. 6a–7a, the crack path clearly connects surface features, some of which are pores.

4. Discussion

The present work concerns the static and dynamic flexural strength of a commercial 99.5% alumina. Here, the surface condition (roughness) is systematically varied to single out the surface roughness influences on the flexural strength. A new methodology was applied for dynamic strength measurements (Belenky and Rittel, 2011). The measured static flexural strength of the investigated material is somewhat lower that the values reported by the manufacturer (Table 1), yet in very good agreement with a previous study on similar grade of alumina (Belenky and Rittel, 2012). The present study showed that there is only a weak minor correlation between static flexural strength and surface roughness. This observation supports an earlier observation of Liao et al. (1997) who reported for their two grades of 99.5% alumina an increase (up to ~25%) in measured strength for better surface finish. For another advanced ceramic material, silicon nitride, it was shown that there is ~30% increase in static flexural strength for a smoother surface finish (Ra 0.02 μm) (Zheng et al., 2000).

Comparison of the static and dynamic flexural strength values reveals one more time (Belenky and Rittel, 2012) a

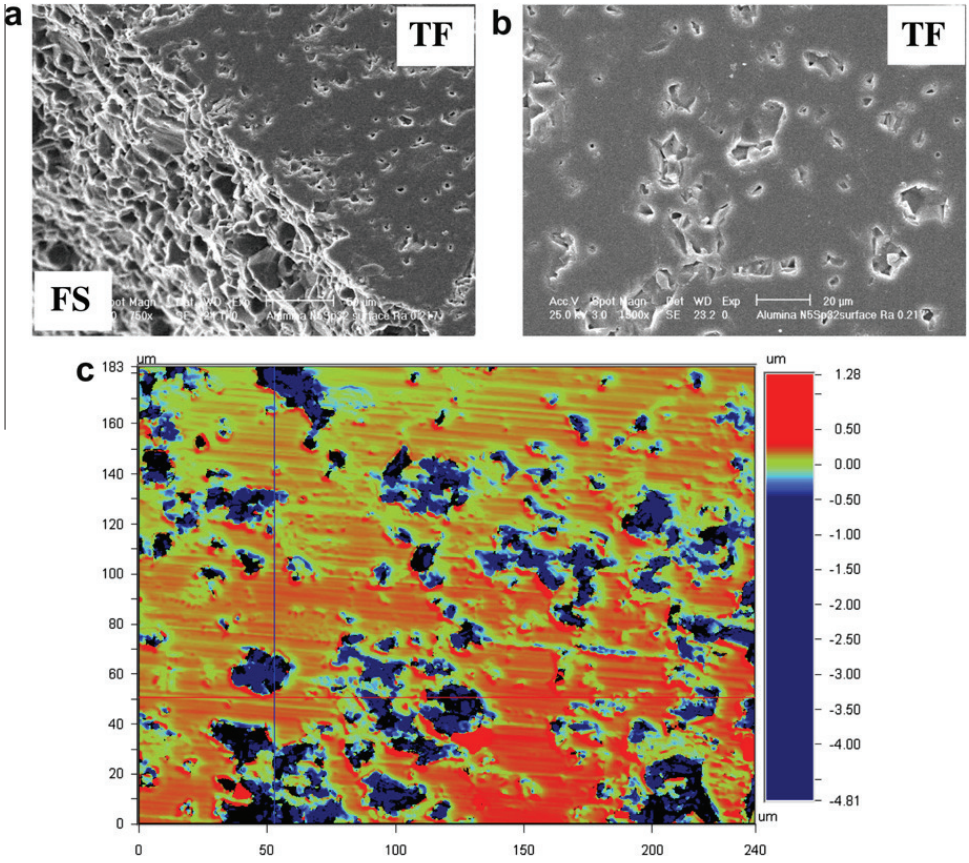

Fig. 6. SEM and optical profilometer images of specimen's surface treatment (polishing) to a level of Ra 0.217 μm. TF stands for a tensile face, FS is a fracture surface: (a) Close up on the tensile face and the fracture surface (SEM, ×750), (b) Surface features left after polishing the specimen to a Ra level of 0.217 μm (SEM, ×1500) and (c) Surface features map as was identified by optical profilometer, the color bar range is from 1.28 to −4.81 μm (×25.7).

significant rate-sensitivity for this material. The observed rate-sensitivity of the investigated brittle material, although surprising at first sight, has been recently reported in the literature for similar material and other brittle materials (Delvare et al., 2010; Nie et al., 2010, 2009). Another claim for the rate-sensitivity of ceramic materials can be found in Zhou and Molinari (2004, 2005). Although of a purely numerical nature, these works explain the rate-sensitivity of ceramics material by showing differences in micro-cracking mechanisms, which operate in static and dynamic loadings. Yet, because of the lack of dynamic tensile strength data for brittle material, Zhou and Molinari (2004, 2005) were not able to further validate it. However, the measured dynamic strength values are highly scattered, to a point that no meaningful statistics can be established. However, it clearly appears that the surface roughness has little or no influence in the range of loading-rates applied in this work to this commercial alumina.

The fractographic study reveals that the failure mechanism in both loading regimes is predominantly transgranular with minor pullouts areas, as shown in Fig. 3. This observation was already reported by other authors, for example Gálvez et al. (2000). No fracture origins can be identified, except for the dynamically broken specimens with low strength values, for which in most of the cases a critical flaw was identified, as shown in Fig. 4. For all loading regimes, a significant level of porosity is observed, both on the fracture surface and on the surfaces of the specimen, irrespective of its roughness. Indeed, the SEM pictures of tensile faces of specimens with different roughness conditions, shown in Figs. 5–7b, reveal that for all roughness conditions pores are present on the tensile faces. Even after polishing (Fig. 7b), pores are clearly present on the tensile face, very similar to a metallographic section from a previous work, Fig. 8. Therefore, it appears that the fracture process is dominated by the presence of surface flaws. These flaws are not obliterated by the polishing process since they are just bulk flaws that appear on the surface, and the more one polishes the surface, the more additional pores are revealed. However, the presence of pores is seldom specifically addressed in the literature. Considering static loading of silicon nitride specimens reported by Zheng et al. (2000), such pores do not appear on the SEM pictures reported. At the same time, these authors report an increase in flexural strength of up to 30%. While the literature about the dynamic loading is scarce, one can refer to the recent work of Nie et al. (2009) who report a significant increase in the dynamic flexural strength of borosilicate glass for smoother surface conditions. Here too, the investigated glass contains no visible surface or bulk flaws of the kind observed in the present work.

One can therefore conclude that the surface roughness condition alone is not always sufficient to control/improve

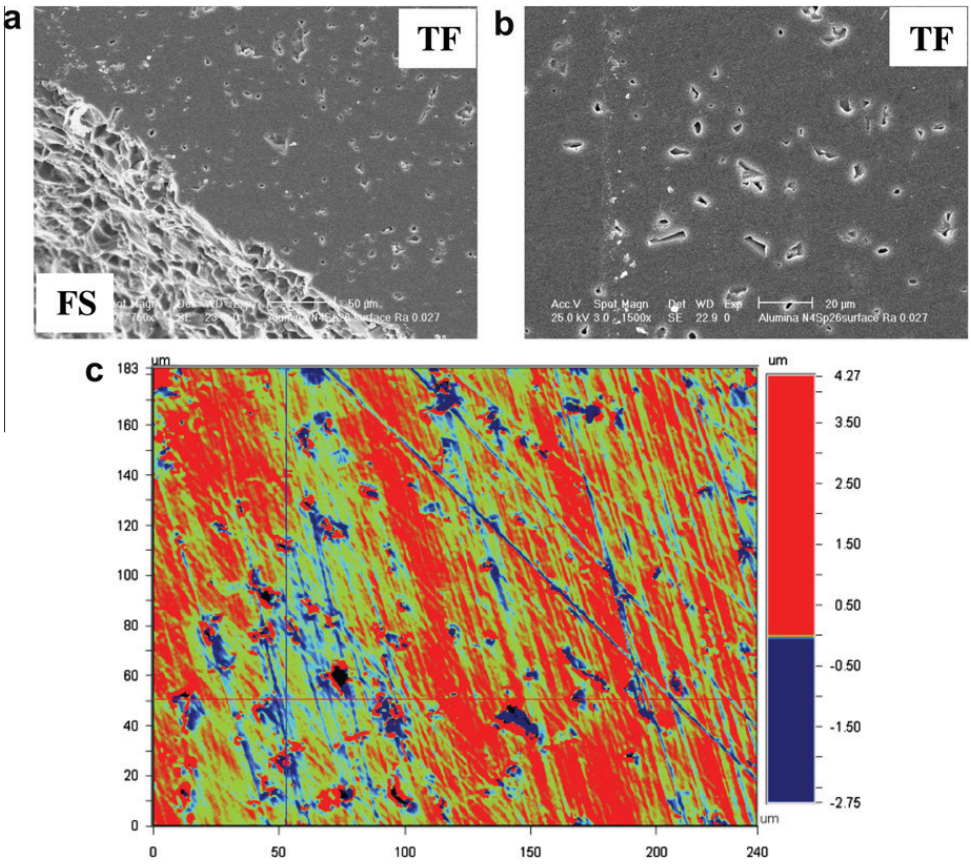

Fig. 7. SEM and optical profilometer images of specimen's surface treatment (polishing) to a level of Ra 0.027 μm. TF stands for a tensile face, FS is a fracture surface: (a) Close up on the tensile face and the fracture surface (SEM, ×750), note that fracture follows surface features, (b) Surface features left after polishing the specimen to a Ra level of 0.027 μm (SEM, ×1500), and (c) Surface features map as was identified by optical profilometery, the color bar range is from 4.27 to −2.75 μm (×25.7).

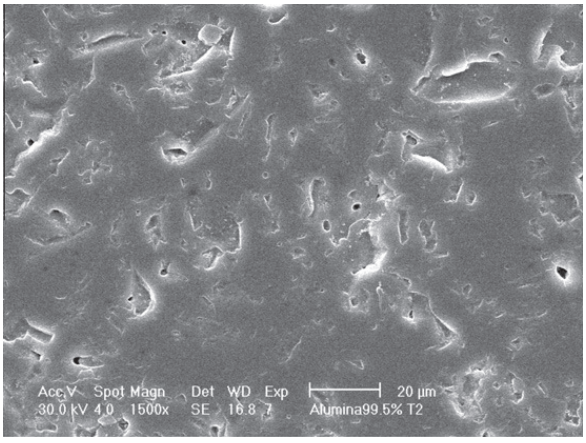

Fig. 8. Polished metallographic section of alumina 99.5% (CoorsTek, USA). Note the virtual similarity of this image to images of polished surfaces (Fig. 6b and Fig. 7b) in terms of porosity.

the flexural strength of advanced ceramics, in both static and dynamic loading conditions. The microstructure, specifically flaws (pores) have a significant effect on the strength, since such flaws are not obliterated during the polishing process. This point is usually not addressed in the literature dealing with the dynamic tensile strength of brittle materials, and apparently contradictory results obtained on different materials can now be all cast into one logical framework, provided microstructural aspects are considered aside the mechanical characterization.

5. Conclusions

The static and dynamic flexural strength of commercial 99.5% alumina was measured on specimens that all had a varying surface roughness condition. The main conclusions of this study are as follows:

1. There is ∼10% increase in static flexural strength of the investigated material for a lower Ra values.
2. For dynamic loading there is no apparent increase in flexural strength for lower Ra values, despite the significant scatter in the results.
3. The investigated material is distinctly rate-sensitive, a point that is in a very good agreement with previous work on a similar material.
4. The failure process is dominated by the presence of bulk flaws (pores) that are natively present in this material. These flaws create local stress concentrations on the tensile face of the specimens, and they are not obliterated by the polishing process. This explains the observed lack of influence of the surface roughness.

5. Contradictory results on the influence (or lack of) of the surface roughness on the strength of various advanced materials can be reconciled by examining the microstructure, specifically the presence or absence of flaws (pores). For those materials without apparent flaws (e.g. glasses), the polishing process is definitely beneficial, while for materials such as the current commercial alumina, improving the surface roughness does not contribute to improve the strength.

Acknowledgements

The authors acknowledge with gratitude Plasan's (Sasa, Israel) financial support through Grant 2013708. Useful discussions with Dr. L. Levin are acknowledged.

References

ABAQUS, 2010. 6.10 ed. Dassault Systems.
Albakry, M., Guazzato, M., Swain, M.V., 2004. Effect of sandblasting, grinding, polishing and glazing on the flexural strength of two pressable all-ceramic dental materials. J. Dent. 32, 91–99.
ASTM-C1161, 1994. Standard test method for flexural strength of advanced ceramics at ambient temperature.
ASTM-C1322, 2005. Standard practice for fractography and charcterization of fracture origins in advanced ceramics.
Bandyopadhyay, B.P., 1995. The effects of grinding parameters on the strength and surface finish of 2 silicon-nitride ceramics. J. Mater. Process. Technol. 53, 533–543.
Belenky, A., Bar-On, I., Rittel, D., 2010. Static and dynamic fracture of transparent nanograined alumina. J. Mech. Phys. Solids 58, 484–501.
Belenky, A., Rittel, D., 2011. A simple methodology to measure the dynamic flexural strength of Brittle materials. Exp. Mech. 51, 1325–1334.
Belenky, A., Rittel, D., 2012. Static and dynamic flexural strength of 99.5% alumina: relation to porosity. Mech. Mater. 48, 43–55.
Bohme, W., Kalthoff, J.F., 1982. The behavior of notched bend specimens in impact testing. Int. J. Fract. 20, R139–R143.
Delvare, F., Hanus, J.L., Bailly, P., 2010. A non-equilibrium approach to processing Hopkinson bar bending test data: application to quasi-brittle materials. Int. J. Impact Eng. 37, 1170–1179.
Gálvez, F., Rodríguez, J., Sánchez-Gálvez, V., 2000. Influence of the strain rate on the tensile strength in aluminas of different purity. J. Phys. IV 10, 323–328.
Guazzato, M., Albakry, M., Quach, L., Swain, M.V., 2004. Influence of grinding, sandblasting, polishing and heat treatment on the flexural strength of a glass-infiltrated alumina-reinforced dental ceramic. Biomaterials 25, 2153–2160.
Gupta, T.K., 1980. Strengthening by surface damage in metastable tetragonal zirconia. J. Am. Ceram. Soc. 63, 117–117.
Holmquist, T.J., Johnson, G.R., 2011. A computational constitutive model for glass subjected to large strains high strain rates and high pressures. J. Appl. Mech. Trans. ASME 78.
Kalthoff, J.F., 1986. Fracture-behavior under high-rates of loading. Eng. Fract. Mech. 23, 289–298.
Kolsky, H., 1949. An investigation of the mechanical properties of materials at very high rates of loading. Proc. Phys. Soc. Sec. B 62, 676–700.
Liao, T.W., Li, K., Breder, K., 1997. Flexural strength of ceramics ground under widely different conditions. J. Mater. Process. Technol. 70, 198–206.
Nakamura, S., Tanaka, S., Kato, Z., Uematsu, K., 2009. Strength-processing defects relationship based on micrographic analysis and fracture mechanics in alumina ceramics. J. Am. Ceram. Soc. 92, 688–693.
Nie, X., Chen, W.N.W., Templeton, D.W., 2010. Dynamic ring-on-ring equibiaxial flexural strength of borosilicate glass. Int. J. Appl. Ceram. Technol. 7, 616–624.
Nie, X., Chen, W.N.W., Wereszczak, A.A., Templeton, D.W., 2009. Effect of loading rate and surface conditions on the flexural strength of borosilicate glass. J. Am. Ceram. Soc. 92, 1287–1295.
Ritter, J.E., Davidge, R.W., 1984. Strength and its variability in ceramics with particular reference to alumina. J. Am. Ceram. Soc. 67, 432–437.
Vlasov, A.S., Zilberbrand, E.L., Kozhushko, A.A., Kozachuk, A.I., Sinani, A.B., 2002. Behavior of strengthened glass under high-velocity impact. Strength Mater. 34, 266–268.
Weisbrod, G., Rittel, D., 2000. A method for dynamic fracture toughness determination using short beams. Int. J. Fract. 104, 89–103.
Zheng, Y.S., Vieira, J.M., Oliveira, F.J., Davim, J.P., Brogueira, P., 2000. Relationship between flexural strength and surface roughness for hot-pressed Si3N4 self-reinforced ceramics. J. Eur. Ceram. Soc. 20, 1345–1353.
Zhou, F., Molinari, J.-F., 2004. Stochastic fracture of ceramics under dynamic tensile loading. Int. J. Solids Struct. 41, 6573–6596.
Zhou, F., Molinari, J.-F., 2005. On the rate-dependency of dynamic tensile strength of a model ceramic system. Comput. Methods Appl. Mech. Eng. 194, 1693–1709.